Prediction of live formation water densities from petroleum reservoirs with pressure-dependent seawater density correlations

Wilson Antonio Cañas-Marín [a] & Andrea Paola Sánchez-Pérez [b]

[a] Centro de Innovación y Tecnología ICP, ECOPETROL, Piedecuesta, Colombia. wilson.cmarin@ecopetrol.com.co
[b] Facultad de Ingenierías Físico-químicas, Universidad Industrial de Santander, Bucaramanga, Colombia. apsanper@uis.edu.co

Abstract
We studied two density correlations developed for seawater at high pressures as potential models to predict formation water densities from petroleum reservoirs as a function of salinity, pressure, gas content, and temperature. The correlations were tested against experimental densities measured at high pressures for live formation waters sampled under bottomhole conditions from five petroleum reservoirs. As a result, one of these seawater correlations was found to be particularly promising to predict formation water densities for these samples, even out of the pressure range originally reported for such a model.

Keywords: salinity; density; live formation water; seawater; reservoir conditions.

Predicción de densidades de aguas vivas de formación de yacimientos petroleros a partir de correlaciones dependientes de presión para densidades de aguas de mar

Resumen
Estudiamos dos correlaciones de densidad desarrolladas para aguas de mar a altas presiones como modelos potenciales para predecir densidades de aguas de formación de yacimientos petroleros en función de salinidad, presión, contenido de gas y temperatura. Las correlaciones fueron probadas contra densidades experimentales, medidas a altas presiones, para aguas vivas de formación muestreadas en condiciones de fondo de pozo. Como resultado se encontró que una de estas correlaciones de agua de mar era particularmente prometedora para predecir las densidades de agua de formación para estas muestras, incluso fuera del rango de presión originalmente reportado para dicho modelo.

Palabras clave: salinidad; densidad; aguas vivas de formación; agua de mar; condiciones de yacimiento.

1. Introduction

Among the most relevant aspects related to the simultaneous production of crude and formation waters (brines) in petroleum reservoirs are the mutual solubility of gas and water, the volumetric changes of both kinds of fluids, and the potential presence of hydrates precipitated due to low temperatures [1]. Brine production increases when the reservoir pressure drops [2]. Aquifers, which are rocks containing water, play a prominent role as an effective tool to recover hydrocarbons from reservoirs, assist the hydrocarbon production in various ways such as: peripheral water drive, edge water drive, and bottom water drive [3]. Moreover, before the production process of a petroleum reservoir, to locate the water-oil contact (WOC) is key in terms of calculating oil reserves. This WOC is particularly difficult to determine when the formation water and the associated crude oil have similar densities. Thus, to experimentally measure live formation water densities under reservoir temperature and pressure conditions makes it

possible to reduce the uncertainty in locating these WOCs. However, samples of formation waters obtained under bottomhole conditions are not usually available, and to have, in this case, a predictive tool based on a few measurements under ambient conditions to predict the formation water densities is very useful. The live formation water densities depend on temperature, pressure, total dissolved solids (TDS), composition, and amount of dissolved gases. The TDS concentration in brines from petroleum reservoirs, made-up mainly of sodium chloride (NaCl), is usually in the range of 1000 to 400000 parts per million (ppm) [4]. In contrast, the seawater salinity is $\cong$ 30000 ppm [1]. The amounts of dissolved gases in formation waters, known as gas-water ratios (GWRs), are commonly less than 30 SCF/STB (i.e., 5.34 m3/m3) [1]. In fact, these values are even lower for the formation waters experimentally measured as part of the present work, proceeding from five Colombian petroleum reservoirs sampled under bottomhole conditions. As demonstrated below, these low GWR values have no effect on the formation water densities measured under reservoir conditions.

Several brine properties such as density, compressibility, and viscosity have attracted attention, and several studies have been conducted regarding these properties [5]. The properties mentioned above can be obtained through different approaches including laboratory experiments [5], available models and correlations [5], and soft computing methods [3]. Currently, laboratory studies are recognized as the most solid and precise method. However, this approach is expensive and time consuming [3], and, as mentioned earlier, samples of formation waters obtained under bottomhole conditions are not usually available. Thus, in the absence of laboratory experiments, other methods such as implementing empirical models and correlations have been used to determine brine properties [3, 5, 6]. In fact, researchers have attempted to provide precise knowledge about the PVT properties of brine in order to apply them in computations together with other important parameters [5]. Most studies, however, use experimental or thermodynamic models that require a great deal of time and calculations [3].

This manuscript is organized as follows: first, two pressure-dependent correlations published in the literature for seawater density calculations are discussed as potential models to predict brine densities from petroleum reservoirs. Then, the two seawater models are tested by using experimental data of (dead and live) formation water densities measured with different salt concentrations and GWRs, measured for this purpose under reservoir conditions for five Colombian petroleum reservoirs. Finally, the main conclusions of this work are presented.

2. Models to predict brine densities

As mentioned earlier, the approach used in the present work was to study the potential application of seawater correlations to predict densities for formation waters coming from petroleum reservoirs. Sharqawy et al. [7] reviewed the existing correlations for predicting thermophysical properties of seawater, and found that most of these correlations, applicable to seawater density calculations, are a function of the temperature and salinity, but these can only be used at atmospheric pressure. However, there are some models for predicting seawater densities including pressure effects. For instance, Millero et al. [8] developed a high-pressure equation of state for water and seawater from experimental data. This model is presented in eq. (1).

$$\rho(S,T,P) = \frac{\rho(S,T,0)}{1 - \dfrac{P}{K(S,T,P)}} \tag{1}$$

Here, $\rho(S,T,0)$ is the standard seawater density at atmospheric pressure, and $K(S,T,P)$ is the secant bulk modulus of the seawater (brine). S, T, and P stand for salinity, temperature, and pressure, respectively. For completeness, the details of this model are presented in Appendix A. Table 1 depicts the salinity, pressure, and temperature ranges given by Millero et al., [8] at which the correlation is valid.

Nayar et al. [9] also developed a model to calculate seawater properties, including the effects of pressure, salinity, and temperature, eq. (2) presents this model:

$$\rho_{sw}(T,S,P) = \rho_{sw}(T,S,P_o) * F_P \tag{2}$$

Here, $\rho_{sw}(T,S,P_o)$ is the seawater density at atmospheric pressure calculated using Sharqawy et al. [7], and F_P is the pressure correction factor. All the remaining mathematical terms for this model are also depicted in Appendix A.

Table 2 shows the salinity, pressure, and temperature ranges of application given by Nayar et al. [9].

Comparing Tables 1 and 2 reveals that the Millero et al. [8] correlation covers a much wider range of pressure conditions than the Nayar et al. [9] model, but the contrary occurs for the temperature conditions, where the range of temperatures for the Nayar et al. model is much higher than the range for the Millero et al. one. With respect to salinity concentrations, both models are for seawater, meaning that in principle these correlations should not be used for salt concentrations superior to 40, and 150 g/kg, respectively.

Table 1.
Salinity, pressure, and temperature ranges for the Millero et al. equation [8].

Salinity (g/kg)	Pressure (MPa)	Temperature (°C)
0	10 - 100	-4 - 40
5	10 - 100	0 - 40
10	10 - 100	0 - 40
15	10 - 100	-2 - 40

Source: Adapted from Millero et al., 1980.

Table 2.
Salinity, pressure, and temperature ranges for the Nayar et al. model [9]

	Salinity (g/kg)	Pressure (MPa)	Temperature (°C)
Primary data	0 – 150	0.1 – 1	0 – 180
	0 – 56	0.2 – 12	0 – 180
Extrapolation	56 – 150	0 – 12	0 – 180

Source: Adapted from Nayar et al., 2016

Table 3.
Experimental data and temperature and pressure ranges used to test seawater models

Formation Water	Salinity (g/kg)	Pressure (MPa)	Temperature (°C)	GWR (scf/STB)
FW1	1.771	3.44 – 27.58	87.77 – 98.88	3.6
FW2	2.268	3.44 – 27.58	87.77 – 98.88	3.5
FW3	17.593	3.44 – 27.58	60 – 104.44	9.5
FW4	3.309	3.44 – 27.58	60 – 104.44	4.9
FW5	8.164	3.44 – 27.58	60 – 104.44	7.4

Source: The Authors

3. Materials and methods

For this work, sets of experimental data for formation water densities were measured for five live formation waters, and used to test the two seawater models presented above. The experimental data and their pressure and temperature ranges are presented in Table 3. This table also shows the salinities and gas-water ratios (GWR) for the five live formation waters.

The experimental density data was obtained by using the Anton Paar high-pressure density meter named as DMA HP 4500/5000®, previously calibrated by following the procedure recommended in the technical manual for this equipment, which can be found elsewhere [10].

4. Results and discussion

The performance of the two seawater models described above were tested against the experimental data of formation water densities measured in the present work. As seen in

Table 4, the density estimations obtained using the Nayar et al. [9] model are found to be in excellent agreement with the experimental data. In fact, its performance is superior to the Millero et al. model [8]. The average error being 0.0669 for Nayar et al, and 0.5544% for Millero et al., respectively. Moreover, although the Nayar et al. model was developed for pressures up to 12 MPa, it behaves very well even for pressures close to 28 MPa. In part, this is due to the linear trend of density versus pressure exhibited by the experimental measurements.

Figs. 1-5 depict details of the performance of the Nayar et al. [9] model for the five formation waters modeled in the present work. The numerical details for the five live and dead formation waters are presented in Appendix B (Tables 1-5).

Table 4.
Relative performance of seawater models against experimental data of formation water densities.

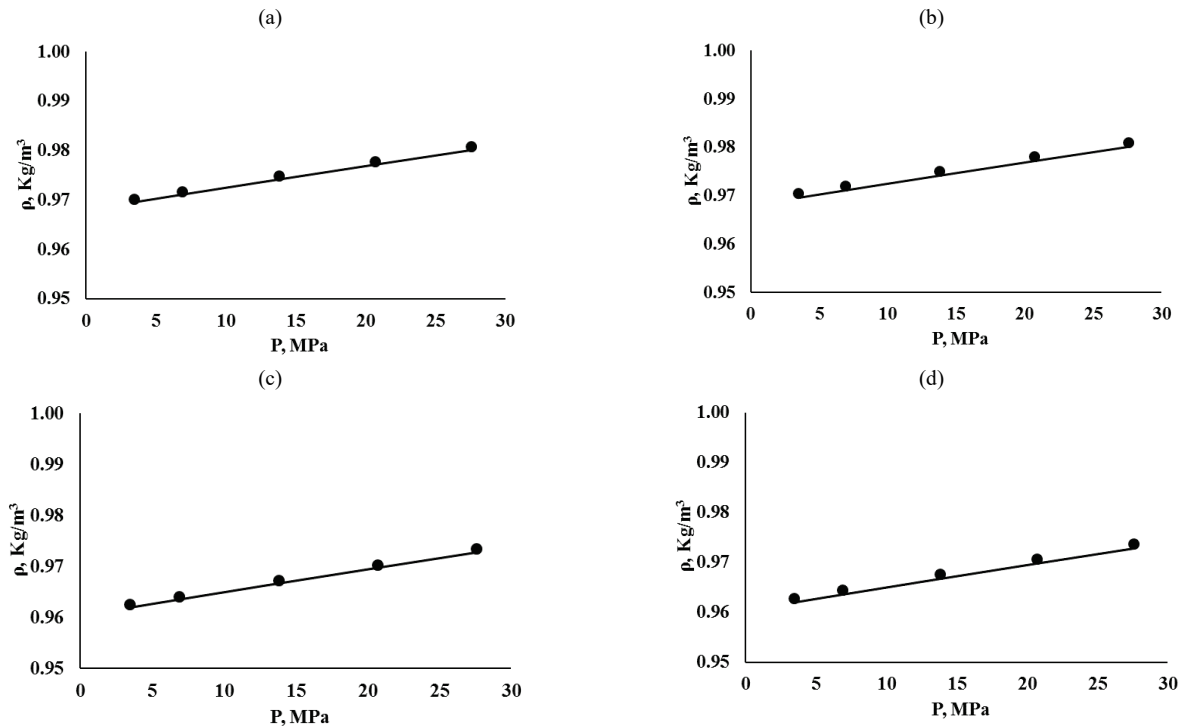| Formation Water	State	Relative Error % (Nayar et al. [9])	Relative Error % (Millero et al. [8])
FW1	live	0.0709	0.6192
	dead	0.0972	0.5926
FW2	live	0.0858	0.5775
	dead	0.1028	0.5603
FW3	live	0.0970	0.3357
	dead	0.0323	0.3297
FW4	live	0.0106	0.6931
	dead	0.0418	0.6747
FW5	live	0.0587	0.5805
	dead	0.0721	0.5804
Overall Average Error %		0.0669	0.5544

Source: The Authors

Figure 1. Water formation densities for FW1. (a) T=87.77°C. Live (b) T=87.77°C. Dead (c) T=98.88°C. Live. (d) T=98.88°C. Dead. Nayar et al. [9] model.
Source: The Authors.

Figure 2. Water formation densities for FW1. (a) T=87.77°C. Live (b) T=87.77°C. Dead (c) T=98.88°C. Live. (d) T=98.88°C. Dead. Nayar et al. [9] model.
Source: The Authors.

Figure 3. Water formation densities for FW1. (a) T=87.77°C. Live (b) T=87.77°C. Dead (c) T=98.88°C. Live. (d) T=98.88°C. Dead. Nayar et al. [9] model.
Source: The Authors.

Figure 4. Water formation densities for FW1. (a) T=87.77°C. Live (b) T=87.77°C. Dead (c) T=98.88°C. Live. (d) T=98.88°C. Dead. Nayar et al. [9] model.
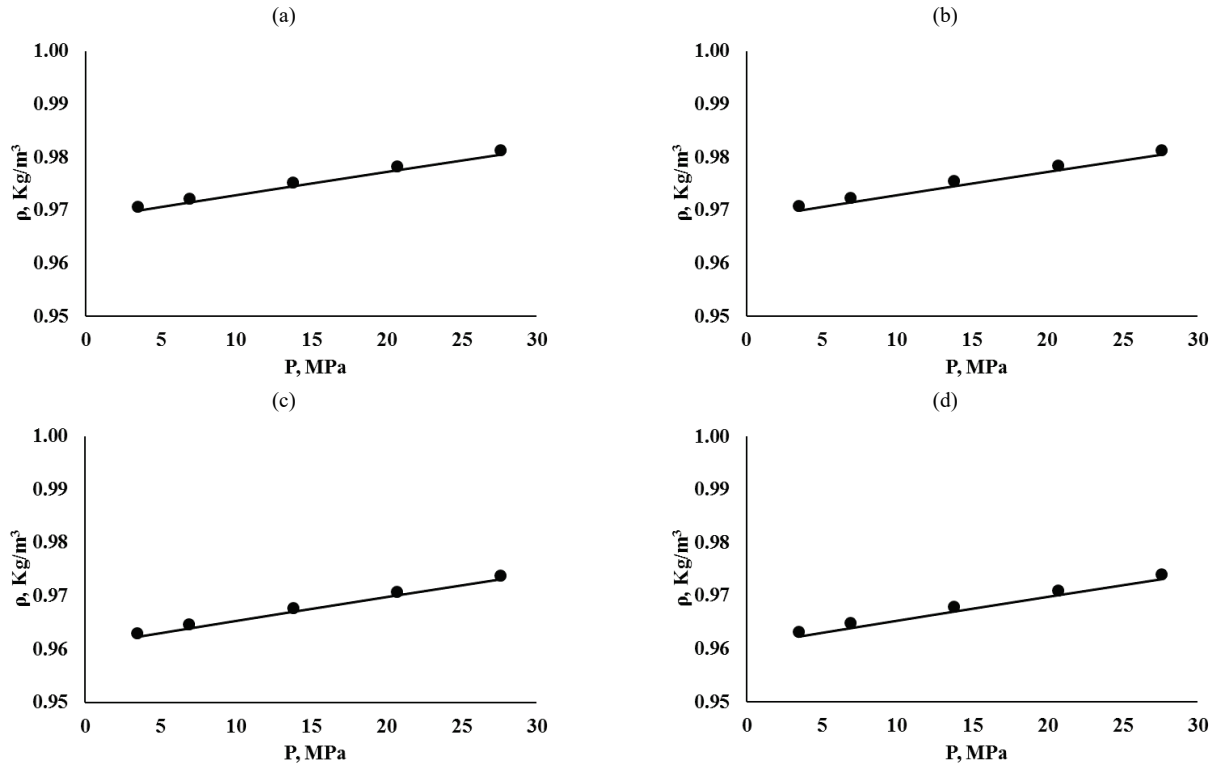Source: The Authors.
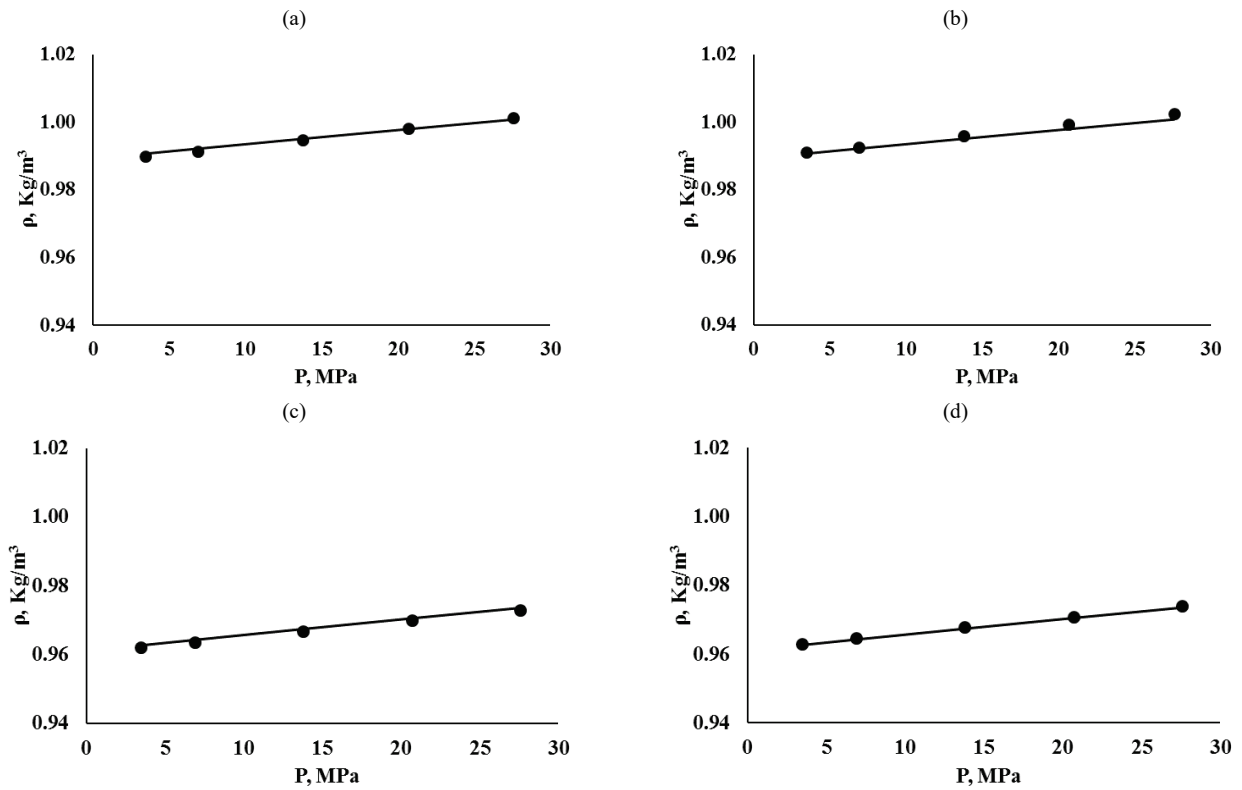
Figure 5. Water formation densities for FW1. (a) T=87.77°C. Live (b) T=87.77°C. Dead (c) T=98.88°C. Live. (d) T=98.88°C. Dead. Nayar et al. [9] model.
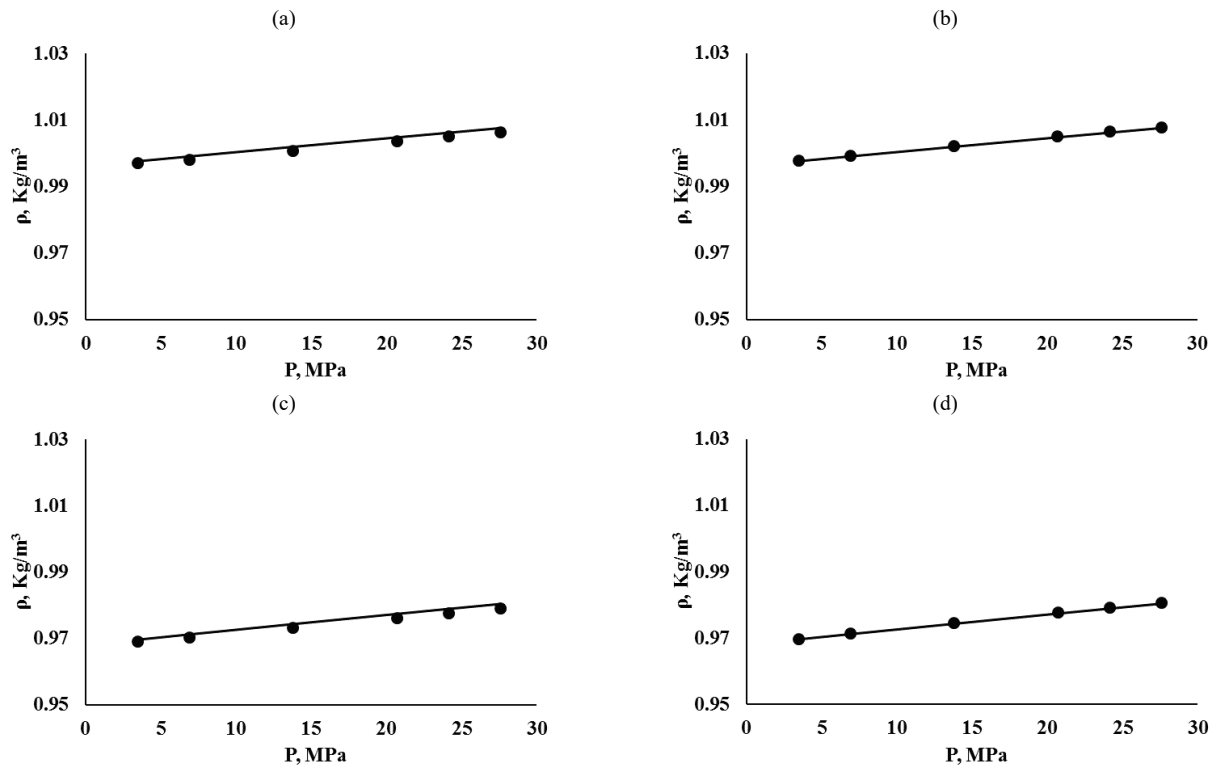Source: The Authors.
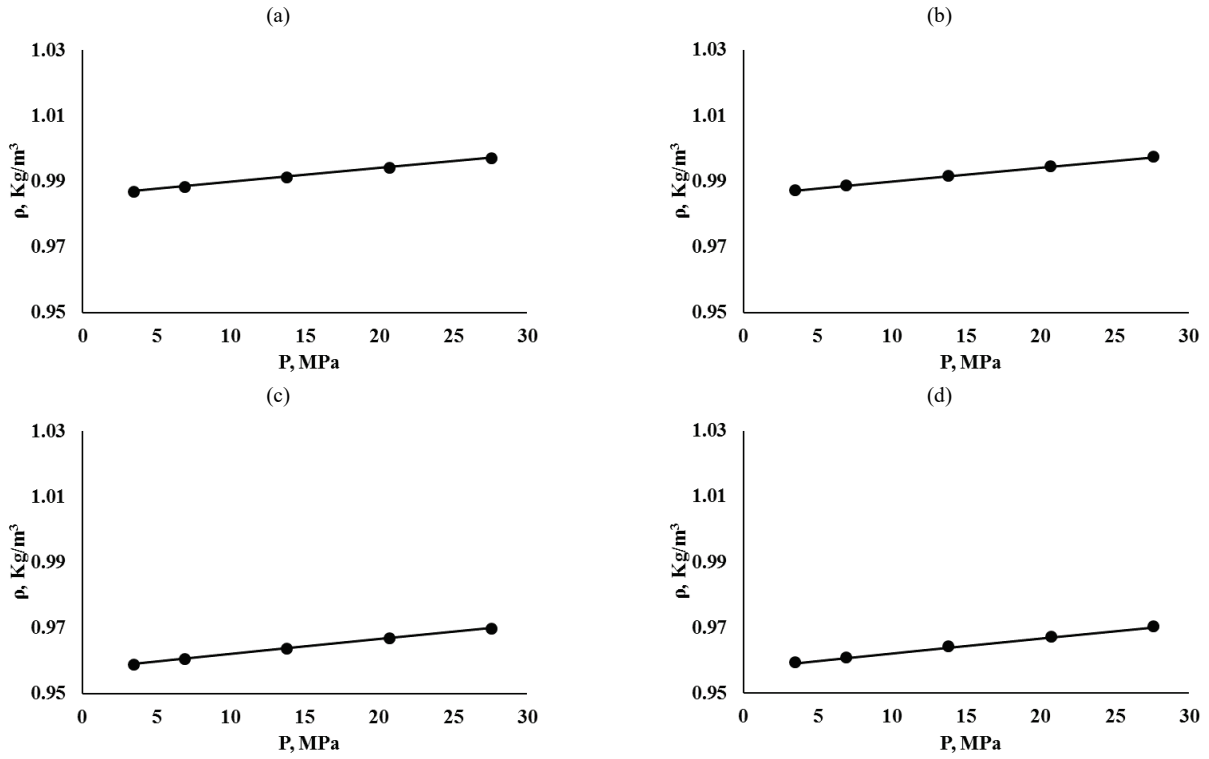
Again, the performance of the Nayar et al. [9] model is excellent. In addition, we can see based on Figures 1-5 that the amounts of gas in these formation waters do not affect the density measurements when compared to the respective dead formation waters. This is due, in part, to the relatively small GWRs values for these brines.

5. Conclusions

The application of pressure-dependent seawater models to predict formation water properties at high pressures can offer rapid estimations of formation water densities for petroleum engineering calculations, such as locating WOCs. This approach is very useful, especially when live formation water samples are not available to perform direct measurements in a PVT laboratory. For the samples modeled here, the gas-water ratio effect (GWR) on the live formation water was insignificant, mainly due to the low values of GWR found for these five live formation water samples. The performance of the Nayar et al. [9] model is excellent for predicting water formation densities, even out of the pressure range originally set for this model. This fact is intimately related to the linear trend of density versus pressure exhibited by the water formations.

Acknowledgments

References

[1] Whitson, C. and Brulé, M., Phase behavior, SPE monograph series, Richardson Texas, USA, 2000.

[2] Bailey, B., Crabtree, M., Tyrie, J., Elphick, J., Kuchuk, F., Romano, C. and Roodhart, L., Water control. Oilfield Review, 12, pp. 30-51, 2000.

[3] Arabloo, M., Shokrollahi, A., Gharagheizi, F. and Mohammadi, A., Toward a predictive model for estimating dew point pressure in gas condensate systems. Fuel Process. Technology 116, pp. 317-324, 2013. DOI: 10.1016/j.fuproc.2013.07.005

[4] Guerra, K., Dahm, K. and Dundorf, S., Oil and gas produced water management and beneficial used in the western United States, Science and Technology Program Report No. 157. Bureau of Reclamation. US Department of Interior, USA, 2011.

[5] Spivey, J. and McCain Jr, W., Estimating density, formation volume factor, compressibility, methane solubility, and viscosity for oilfield brines at temperatures from 0 to 275 °C, pressures to 200 Mpa, and salinities to 5.7 mole/kg. JCPT, 43(7), pp. 52-61, 2004.

[6] Tatar, A., Naseri, S., Sirach, N., Lee, M. and Bahadori, A., Prediction of reservoir brine properties using radial basis function (RBF) neural network, Petroleum, 1(4), pp. 349-357, 2015. DOI: 10.1016/j.petlm.2015.10.011.

[7] Sharqawy, M., Lienhard, J. and Zubair, S., Thermophysical properties of seawater: a review of existing correlations and data. Desalination and Water Treatment, 16, pp. 354-380., 2010. DOI: 10.5004/dwt.2010.1079.

[8] Millero, F.J., Chen, C.T., Bradshaw, A. and Schleicher, K., A new high-pressure equation of state for seawater, Deep Sea Research Part A, Oceanographic Research Papers. 27(3-4), pp. 255-264, 1980. DOI: 10.1016/0198-0149(80)90016-3

[9] Nayar, K., Sharqawy, M., Banchik, L. and Lienhard, J., Thermophysical properties of seawater: a review and new correlations

that include pressure dependence. Desalination, 390, pp. 1-24, 2016. DOI: 10.1016/j.desal.2016.02.024.

[10] Instruction Manual DMA 4500/5000, Denstiy/ Specific Gravity/ Concentation Meter. Software Version V5.012.c, Anton Paar, 2005.

W.A. Cañas-Marín, completed his BSc. in 1997 from the Universidad de Antioquia, Medellin, Colombia and MSc. in 2002 from the Universidad Industrial de Santander, Colombia, both in Chemical Engineering. He is currently a chemical Engineer at ECOPETROL, S.A.'s, Instituto Colombiano del Petróleo-ICP. His research interests include thermodynamic characterization of reservoir fluids and phase behavior modeling, effects of external fields on matter, molecular simulation, and flow assurance.
ORCID: 0000-0002-3670-1779.

A.P. Sánchez-Pérez, completed her BSc. in Systems Engineering in 2003, and Sp. in Telecommunications in 2010, both of them from the Universidad Industrial de Santander, Bucaramanga, Colombia. Since 2005, she has been working for oil and gas consulting companies in the characterization of reservoir fluids, phase behavior modeling, and EOR modeling. Currently, she is a co-investigator for the Universidad Industrial de Santander-ECOPETROL cooperation agreement. Her areas of interest include phase behavior modeling and heavy oil reservoir characterization.
ORCID: 0000-0003-4564-1891.

List of symbols

ρ: formation water density, kg/m3
T: temperature, °C
P: pressure, MPa
S: salinity, g/kg
sw: seawater

Appendix A

A.1. High pressure Equation of state for seawater, Millero et al [8].

The density of seawater at high pressure according to the equation of state for seawater (EOS-80) is calculated as presented in eq. (3):

$$\rho(S,T,P) = \frac{\rho(S,T,0)}{1 - \frac{P}{K(S,T,P)}} \tag{3}$$

Where $\rho(S,T,0)$ is the density of standard seawater at atmospheric pressure and is calculated as shown in eq. (4), P is pressure in bars and $K(S,T,P)$ is the secant bulk modulus of seawater and is calculated with eq. (5).

- Density of standard seawater at atmospheric pressure:

$$
\begin{aligned}
\rho(S,T,0) = &(0.999841594 + 6.793952*10^{-5}T - \\
&9.095290*10^{-6}T^2 + 1.001685*10^{-7}T^3 - \\
&1.120083*10^{-9}T^4 + 6.536362*10^{-12}T^5) + \\
&(8.25917*10^{-4} - 4.4490*10^{-6}T + 1.0485* \\
&10^{-7}T^2 - 1.2580*10^{-9}T^3 + 3.315* \\
&10^{-12}T^4)S + (-6.33761*10^{-6} + 2.8441* \\
&10^{-7}T - 1.6871*10^{-8}T^2 + 2.83258* \\
&10^{-10}T^3)S^{3/2} + (5.4705*10^{-7} - 1.97975* \\
&10^{-8}T + 1.6641*10^{-9}T^2 - 3.1203* \\
&10^{-11}t^3)S^2
\end{aligned} \tag{4}
$$

- Secant bulk modulus of seawater:

$$K(S,T,P) = K^0 + AP + BP^2 \tag{5}$$

Where:

$$K^0 = K_w^0 + aS + bS^{3/2}$$
$$A = A_w + cS + dS^{3/2}$$
$$B = B_w + eS$$

$$K_w^0 = 19652.21 + 148.4206T - 2.327105T^2 + 1.360477 * 10^{-2}T^3 - 5.155288 * 10^{-5}T^4$$
$$A_w = 3.239908 + 1.43713 * 10^{-3}T + 1.16092 * 10^{-4}T^2 - 5.77905 * 10^{-7}T^3$$
$$B_w = 8.50935 * 10^{-5} - 6.12293 * 10^{-6}T + 5.2787 * 10^{-8}T^2$$
$$a = 54.6746 - 0.603459T + 1.09987 * 10^{-2}T^2 - 6.1670 * 10^{-5}T^3$$
$$b = 7.944 * 10^{-2} + 1.6483 * 10^{-2}T - 5.3009 * 10^{-4}T^2$$
$$c = 2.2838 * 10^{-3} - 1.0981 * 10^{-5}T - 1.6078 * 10^{-6}T^2$$
$$d = 1.9107 * 10^{-4}$$
$$e = -9.9348 * 10^{-7} + 2.0816 * 10^{-8}T + 9.1697 * 10^{-10}T^2$$

Units: ρ in kg/m3, S in kg/m3, T in °C and P in bar.

A.2. Seawater density correlation, Nayar et al. [9].

The density of seawater at high pressure according to Nayar et al. [9] is calculated as shown in eq. (6).

$$\rho_{sw}(T,S,P) = \rho_{sw}(T,S,P_o) * F_P \tag{6}$$

Where $\rho_{sw}(T,S,P_o)$ is the seawater density at atmospheric pressure calculated by using Sharqawy et al. [5] and F_P is the pressure correction factor. The equations to calculate these expressions are shown in eq. (7) and (8) respectively.

$$\rho_{sw}(T,S,P_o) = (a_1 + a_2T + a_3T^2 + a_4T^3 + a_5T^4) + \tag{7}$$
$$(b_1 S_{Kg/Kg} + b_2 S_{Kg/Kg}T + b_3 S_{Kg/Kg}T^2 + b_4 S_{Kg/Kg}T^3 + b_5 S_{Kg/Kg}^2 tT^2)$$

Where:

$a_1 = 9.999 * 10^2$ $b_1 = 8.020 * 10^2$
$a_2 = 2.034 * 10^{-2}$ $b_2 = -2.001$
$a_3 = -6.162 * 10^{-3}$ $b_3 = 1.677 * 10^{-2}$
$a_4 = 2.261 * 10^{-5}$ $b_4 = -3.060 * 10^{-5}$
$a_5 = -4.657 * 10^{-8}$ $b_5 = -1.613 * 10^{-5}$

$$S_{Kg/Kg} = \frac{S}{1000}$$

$$F_p = exp\left[(P - P_o) * X + \frac{(P^2 - P_o^2)}{2} * Y\right] \tag{8}$$

Where:

$$X = c_1 + c_2t + c_3t^2 + c_4t^3 + c_5t^4 + c_6t^5 + S * (d_1 + d_2t + d_3t^2)$$
$$Y = c_7 + c_8t + c_9t^3 + +d_4S$$

$c_1 = 5.0792 * 10^{-4}$ $d_1 = -1.1077 * 10^{-6}$
$c_2 = -3.4168 * 10^{-6}$ $d_2 = 5.5584 * 10^{-9}$
$c_3 = 5.6931 * 10^{-8}$ $d_3 = -4.2539 * 10^{-11}$
$c_4 = -3.7263 * 10^{-10}$ $d_4 = 8.3702 * 10^{-9}$
$c_5 = 1.4465 * 10^{-12}$
$c_6 = -1.7058 * 10^{-15}$
$c_7 = -1.3389 * 10^{-6}$
$c_8 = 4.8603 * 10^{-9}$
$c_9 = -6.8039 * 10^{-13}$

Units: ρ_{sw} in kg/m³, t in °C, S in g/kg, P in MPa

Appendix B

Table B1.
Experimental vs. calculated data for FW1. Salinity= 1.77122 g/kg. Nayar et al. [9] model.

FW1	T (°C)	P (MPa)	Exp. Density (kg/m³)	Calc. Density (kg/m³)	Error (%)	Average Error (%)
Live	87.77	27.579	0.98087	0.98011	0.077	0.071
		20.684	0.97789	0.97716	0.074	
		13.790	0.97488	0.97416	0.074	
		6.895	0.97178	0.97110	0.069	
		3.447	0.97024	0.96955	0.071	
	98.88	27.579	0.97345	0.97275	0.072	
		20.684	0.97040	0.96973	0.068	
		13.790	0.96731	0.96666	0.067	
		6.895	0.96419	0.96352	0.069	
		3.447	0.96257	0.96193	0.067	
Dead	87.77	27.579	0.98110	0.98011	0.101	0.097
		20.684	0.97812	0.97716	0.098	
		13.790	0.97512	0.97416	0.098	
		6.895	0.97206	0.97110	0.099	
		3.447	0.97048	0.96955	0.095	
	98.88	27.579	0.97369	0.97275	0.096	
		20.684	0.97063	0.96973	0.093	
		13.790	0.96759	0.96666	0.096	
		6.895	0.96447	0.96352	0.099	
		3.447	0.96286	0.96193	0.096	

Source: The Authors

Table B2.
Experimental vs. calculated data for FW2. Salinity= 2.268 g/kg. Nayar et al. [9] model.

FW2	T (°C)	P (MPa)	Exp. Density (kg/m³)	Calc. Density (kg/m³)	Error (%)	Average Error (%)
Live	87.77	27.579	0.98134	0.98047	0.089	0.086
		20.684	0.97841	0.97752	0.091	
		13.790	0.97535	0.97452	0.086	
		6.895	0.97230	0.97146	0.086	
		3.447	0.97072	0.96992	0.082	
	98.88	27.579	0.97392	0.97311	0.083	
		20.684	0.97092	0.97010	0.085	
		13.790	0.96778	0.96702	0.078	
		6.895	0.96475	0.96388	0.090	
		3.447	0.96314	0.96230	0.088	
Dead	87.77	27.579	0.98144	0.98047	0.098	0.103
		20.684	0.97855	0.97752	0.105	
		13.790	0.97554	0.97452	0.105	
		6.895	0.97244	0.97146	0.100	
		3.447	0.97090	0.96992	0.102	
	98.88	27.579	0.97411	0.97311	0.103	
		20.684	0.97111	0.97010	0.104	
		13.790	0.96797	0.96702	0.098	
		6.895	0.96490	0.96388	0.105	
		3.447	0.96333	0.96230	0.107	

Source: The Authors

Table B3.
Experimental vs. calculated data for FW3. Salinity= 17.593 g/kg. Nayar et al. [9] model.

FW3	T (°C)	P (MPa)	Exp. Density (kg/m³)	Calc. Density (kg/m³)	Error (%)	Average Error (%)
Live	60	27.579	1.00642	1.00756	0.113	
		24.132	1.00518	1.00616	0.098	
		20.684	1.00375	1.00476	0.101	
		13.790	1.00084	1.00192	0.108	
		6.895	0.99813	0.99904	0.091	
		3.447	0.99706	0.99758	0.052	0.097
	104.44	27.579	0.97922	0.98040	0.120	
		24.132	0.97779	0.97890	0.114	
		20.684	0.97624	0.97739	0.118	
		13.790	0.97326	0.97432	0.109	
		6.895	0.97035	0.97120	0.087	
		3.447	0.96910	0.96961	0.053	
Dead	60	27.579	1.00790	1.00756	0.034	
		24.132	1.00651	1.00616	0.035	
		20.684	1.00509	1.00476	0.033	
		13.790	1.00218	1.00192	0.026	
		6.895	0.99927	0.99904	0.023	
		3.447	0.99788	0.99758	0.029	0.032
	104.44	27.579	0.98078	0.98040	0.039	
		24.132	0.97925	0.97890	0.036	
		20.684	0.97771	0.97739	0.032	
		13.790	0.97467	0.97432	0.036	
		6.895	0.97153	0.97120	0.034	
		3.447	0.96990	0.96961	0.030	

Source: The Authors

Table B4.
Experimental vs. calculated data for FW4. Salinity= 3.309 g/kg. Nayar et al. [9] model.

FW4	T (°C)	P (MPa)	Exp. Density (kg/m³)	Calc. Density (kg/m³)	Error (%)	Average Error (%)
Live	60	27.579	0.99714	0.99725	0.010	
		20.684	0.99433	0.99441	0.007	
		13.790	0.99134	0.99152	0.019	
		6.895	0.98843	0.98859	0.016	
		3.447	0.98699	0.98710	0.011	0.011
	104.44	27.579	0.96995	0.97001	0.006	
		20.684	0.96688	0.96696	0.008	
		13.790	0.96376	0.96384	0.009	
		6.895	0.96058	0.96067	0.009	
		3.447	0.95895	0.95906	0.010	
Dead	60	27.579	0.99762	0.99725	0.038	
		20.684	0.99481	0.99441	0.041	
		13.790	0.99186	0.99152	0.034	
		6.895	0.98891	0.98859	0.033	
		3.447	0.98747	0.98710	0.037	0.042
	104.44	27.579	0.97047	0.97001	0.047	
		20.684	0.96745	0.96696	0.050	
		13.790	0.96433	0.96384	0.050	
		6.895	0.96110	0.96067	0.045	
		3.447	0.95947	0.95906	0.044	

Source: The Authors

Table B5.
Experimental vs. calculated data for FW5. Salinity= 8.164 g/kg. Nayar et al. [9] model.

FW5	T (°C)	P (MPa)	Exp. Density (kg/m³)	Calc. Density (kg/m³)	Error (%)	Average Error (%)
Live	60	27.579	1.00138	1.00075	0.063	
		20.684	0.99806	0.99793	0.013	
		13.790	0.99476	0.99506	0.030	
		6.895	0.99138	0.99214	0.077	
		3.447	0.98994	0.99067	0.074	0.059
	104.44	27.579	0.97293	0.97354	0.063	
		20.684	0.96986	0.97050	0.067	
		13.790	0.96678	0.96741	0.064	
		6.895	0.96355	0.96425	0.072	
		3.447	0.96202	0.96264	0.065	
Dead	60	27.579	1.00253	1.00075	0.177	
		20.684	0.99925	0.99793	0.133	
		13.790	0.99591	0.99506	0.085	
		6.895	0.99253	0.99214	0.039	
		3.447	0.99113	0.99067	0.047	0.072
	104.44	27.579	0.97407	0.97354	0.054	
		20.684	0.97095	0.97050	0.045	
		13.790	0.96787	0.96741	0.048	
		6.895	0.96473	0.96425	0.050	
		3.447	0.96306	0.96264	0.043	

Source: The Authors